J Neurophysiol 90: 2014–2021, 2003.
First published May 21, 2003; 10.1152/jn.00395.2003.

Shaker K^+ Channels Contribute Early Nonlinear Amplification to the Light Response in *Drosophila* Photoreceptors

Mikko Juusola[2], Jeremy E. Niven[2], and Andrew S. French[1]

[1]*Department of Physiology and Biophysics, Dalhousie University, Halifax B3H 4H7, Nova Scotia, Canada; and* [2]*Physiological Laboratory, University of Cambridge, Cambridge, CB2 3EG United Kingdom*

Submitted 21 April 2003; accepted in final form 20 May 2003

Juusola, Mikko, Jeremy E. Niven, and Andrew S. French. *Shaker* K^+ channels contribute early nonlinear amplification to the light response in *Drosophila* photoreceptors. *J Neurophysiol* 90: 2014–2021, 2003. First published May 21, 2003; 10.1152/jn.00395.2003. We describe the contribution of rapidly inactivating *Shaker* K^+ channels to the dynamic membrane properties of *Drosophila* photoreceptors. Phototransduction was measured in wild-type and *Shaker* mutant (Sh^{14}) *Drosophila* photoreceptors by stimulating with white noise– modulated light contrast and recording the resulting intracellular membrane potential fluctuations. A second-order Volterra kernel series was used to characterize the nonlinear dynamic properties of transduction in the two situations. First-order kernels were indistinguishable in wild-type and Sh^{14} photoreceptors, indicating that the basic light transduction machinery was always intact. However, second-order kernels of *Shaker* mutants lacked a large, early amplification, indicating a novel role for *Shaker* K^+ channels in amplifying and accelerating the voltage response of wild-type photoreceptors. A cascade model of two nonlinear static components surrounding one linear dynamic component was able to partially reproduce the experimental responses. Parameters obtained by fitting the model to the experimental data supported the hypothesis that normal *Shaker* K^+ channels contribute an early, positive nonlinearity that partially offsets a later attenuating nonlinearity caused by membrane shunting.

INTRODUCTION

A major challenge both in neuroscience and in other integrative disciplines is to determine the normal functions of molecules identified by molecular genetic approaches. Even within single cells, functional studies must cope with complex, often nonlinear, interactions between multiple cellular components. Analyzing such nonlinearities may require detailed knowledge of entire cell function, in addition to the properties of the individual cellular components in question (Kitano 2002). *Drosophila* photoreceptors provide a genetically tractable system in which individual cellular components, including ion channels and sensory transduction proteins can be studied (Hardie 2001; Weckström and Laughlin 1995). Combined with quantitative measures of photoreceptor performance, such as sensitivity, signal-to-noise ratio, and frequency response, as well as behavior (e.g., Schilstra and van Hateren 1999; van Hateren and Schilstra 1999), these cellular and molecular approaches provide a system where the contributions of individual cellular components to normal cell function may be determined (Juusola and Hardie 2001a).

Drosophila and other insect photoreceptors (e.g., Weckström et al. 1991) contain voltage-activated K^+ channels (Hardie 1991) that contribute strongly to photoreceptor membrane behavior and may reflect the insects' visual ecology (Weckström and Laughlin 1995). *Drosophila* photoreceptors express an array of voltage-activated K^+ channels including the rapidly inactivating *Shaker* K^+ channel and at least two noninactivating K^+ channels (Hardie 1991). The *Shaker* K^+ channel in *Drosophila* was the first cloned K^+ channel and has been extensively investigated (Hille 2001), but the roles of *Shaker* and its homologs remain unclear. Suggested functions include the attenuation of graded potentials and back-propagated action potentials in dendrites (Hoffman et al. 1997; Laurent 1990; Magee et al. 1998), modulation of firing frequencies of spiking neurons (Connor and Stevens 1971), and control of spike propagation reliability (Debanne et al. 1997).

Recent work has indicates that *Shaker* increases the dynamic range of phototransduction and improves the signal-to-noise ratio in *Drosophila* photoreceptors (Niven et al. 2003). However, the relationship between this voltage-activated ion channel and membrane potential is inherently nonlinear. To determine the nonlinear contributions of *Shaker* K^+ channels we recorded photoreceptor membrane potentials in wild-type and *Shaker* mutant *Drosophila* during stimulation with wide-bandwidth light fluctuations, and measured the linear and second-order nonlinear components of transduction by a Volterra functional series expansion.

Wild-type photoreceptors demonstrated an early positive nonlinear component that amplified and accelerated the photoresponse, but this component was absent in mutant photoreceptors. Simulation of phototransduction with a nonlinear cascade model supported this conclusion and indicated that *Shaker* K^+ channel adds a nonlinear effect early in the transduction process.

METHODS

Fly stocks

The wild-type strain was red-eyed *Drosophila melanogaster* Oregon Red. The null mutation in the *Shaker* channel, Sh^{14}, a missense mutation in the core region resulting in nonfunctional *Shaker* channels (Kaplan and Trout 1961), was also expressed in red-eyed flies. Both strains of flies were raised at 19°C in darkness.

Address for reprint requests and other correspondence: A. S. French, Department of Physiology and Biophysics, Dalhousie University, Halifax, Nova Scotia B3H 4H7, Canada. (E-mail: andrew.french@dal.ca).

The costs of publication of this article were defrayed in part by the payment of page charges. The article must therefore be hereby marked "*advertisement*" in accordance with 18 U.S.C. Section 1734 solely to indicate this fact.

Recording and stimulation

Flies were fixed with wax into a ceramic holder and a small window was cut into the surface of the compound eye (Juusola and Hardie 2001a). Intracellular recordings were made using quartz microelectrodes, with resistances between 150 and 220 MΩ, filled with 3M KCl. A second blunt microelectrode filled with fly Ringer was also placed in the flies' heads close to the eyes. All recordings were made using an intracellular amplifier (SEC-10L, NPI Electronic, Tamm, Germany) in current-clamp mode using switching frequencies of 8–20 kHz and low-pass filtered at 500 Hz (elliptic). Temperature was maintained at 25°C throughout the experiments to within 1°C accuracy using a custom-built thermocouple feedback to a Peltier device. Photoreceptors were only used if their membrane potential was more negative than −55 mV and they had at least a 45-mV saturating impulse response in dark-adapted conditions. Data acquisition, stimulus generation, and signal analysis were performed by a custom-built MATLAB interface (Juusola and Hardie 2001a).

Photoreceptors were stimulated with a pseudorandom light contrast $x(t)$, generated by a high-intensity green light-emitting diode with peak wavelength 525 nm (Marl Optosource) at a mean intensity of 3×10^6 photons/s. Intensity was extrapolated from the average number of single photon responses to a dim, steady light background counted in the same photoreceptor during 10 s. Background intensity was increased or reduced by neutral density filters between the light source and the eye. All light intensity measurements were converted to dimensionless contrast units with a mean contrast of 0.32. Light intensity and photoreceptor membrane potential were sampled at 1-ms intervals during the presentation of pseudorandomly fluctuating sequences of 100 s duration.

Nonlinear system identification

The original sampling resolution of 1 ms was reduced to 2 ms by combining adjacent points to give records of 50,000 data pairs (light intensity in contrast units and receptor potential in mV). For each record, the first 40,000 data pairs were analyzed as the input and output of an unknown nonlinear dynamic system with light intensity as the input $x(t)$, as a function of time t, and the receptor potential as output $y(t)$, represented by the first 3 terms of a Volterra functional series

$$y(t) = K_0 + \int_{-\infty}^{\infty} K_1(u)x(t-u)\mathrm{d}u + \int_{-\infty}^{\infty}\int_{-\infty}^{\infty} K_2(u, v)x(t-u)x(t-v)\mathrm{d}u\mathrm{d}v \quad (1)$$

where K_0, $K_1(u)$, and $K_2(u, v)$ are the kernels of the system and u, v indicate time lags.

Several methods have been developed for kernel estimation (French and Marmarelis 1999). Earlier methods relied on stimulating the unknown system with Gaussian white noise, or a close approximation, but more recent methods avoid this requirement. The parallel cascade method (Korenberg 1991) is based on the principle that a wide range of nonlinear dynamic systems can be approximated by a parallel cascade of simple nonlinear systems (branches), each consisting of a linear filter followed by a static nonlinearity (Fig. 1). Branches are added one by one, with each chosen to minimize the squared error remaining after subtracting the sum of all the previous branch outputs from the actual system output. Addition of branches proceeds until some predetermined criterion of error level or number of branches is reached.

The choice of linear filters is arbitrary. Filters chosen by cross-correlation between input and output can produce very rapid convergence (French and Marmarelis 1999; Korenberg 1991). We used an alternative approach, where the filters are formed from Gaussian distributed random numbers (French et al. 2001). This method is relatively slow, and often requires $\leq 10^5$ cascade branches, but it is completely general and makes no initial assumptions about the forms

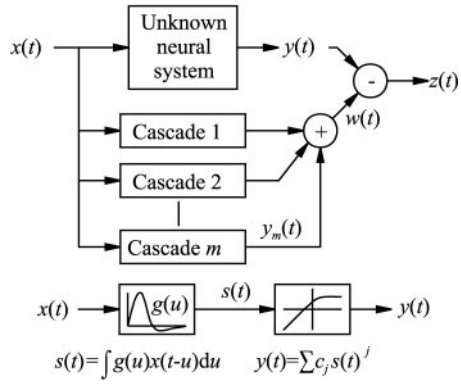

FIG. 1. Parallel cascade scheme for nonlinear system identification. Input signal $x(t)$, where t is time, passes through unknown nonlinear neural system to give output $y(t)$. Cascade of parallel nonlinear branches is formed from set of linear filters $g(u)$, where u is filter time lag, giving filtered outputs $s(t)$, that feed static nonlinear functions [in this case polynomials, $\Sigma c_j s(t)^j$, where c_j are the polynomial coefficients]. Structure of single branch is shown below. Each branch m of cascade has different parameters $g(u)$ and c_j to produce a set of outputs $y_m(t)$. Sum of cascades $w(t)$ is subtracted from unknown system output to give residual signal $z(t)$. Addition of each branch to cascade is chosen to minimize mean squared value of $z(t)$.

of the kernels or the nature of the input or output signals. Modern computing power allows this inefficient, but general and objective method to be easily applied to a wide range of data.

Once each filter is chosen, the polynomial function is calculated by linear regression. Kernels are then updated by adding the filter function multiplied by the appropriate polynomial coefficients. An important feature of the method is that it can be applied to systems containing relatively high-order nonlinearities by extending the polynomial function. However, it is not necessary to construct all of the higher-order kernels. Another important point is that the final number of parameters used to fit the data are given by the kernel values themselves, so a large number of cascade branches does not increase the number of fitted parameters, only their accuracy.

After kernel estimation, percentage mean square error (MSE) values (French and Marmarelis 1999) were calculated for the zero and first-order kernels alone and for the combined, zero-, first-, and second-order kernels from

$$\mathrm{MSE} = 100 \cdot \frac{\overline{[y(t) - y_s(t)]^2}}{\overline{y^2(t)} - [\overline{y(t)}]^2} \quad (2)$$

where $y_s(t)$ is the Volterra series output (*Eq. 1*) and the bars indicate time averages.

The kernel estimates were then substituted into *Eq.1* and used to predict the output of the nonlinear system to the input signal of the remaining 10,000 data pairs of each record. Therefore all predictions were based on data that had not been used for system identification.

Simulation

Nonlinear responses in *Drosophila* photoreceptors were simulated by a NLN (nonlinear static–linear dynamic–nonlinear static) cascade model (French et al. 1993). The two nonlinear components were third-order polynomial functions and the linear component was the Wong and Knight photoreceptor model (Wong et al. 1980)

$$g(t) = \frac{1}{n!\tau}\left(\frac{t}{\tau}\right)^n \mathrm{e}^{-t/\tau} \quad (3)$$

where n and τ are parameters to be fitted. To remove redundant parameters, only one constant term was included in the model, as an offset in the output of the linear component. Similarly, the first nonlinear component had a fixed first-order coefficient of unity. The

numbers of unknown parameters were therefore: 2 (first polynomial) + 3 (Wong and Knight model plus offset) + 3 (second polynomial) = 8. The NLN cascade model was fitted to the same 40,000 data pairs as used for the kernel analysis. Fitting was performed in 2 stages, using simulated annealing to obtain an approximate fit and then the Levenberg–Marquardt method with the simulated annealing results as the starting condition (Press et al. 1990). The fitting algorithms always converged satisfactorily. Mean square errors were again calculated using *Eq.2*.

Data analysis and graphical presentations were performed by custom-written software using the C++ programming language and PC-compatible desktop computers.

RESULTS

We recorded from wild-type *Drosophila* photoreceptors and those with mutation Sh^{14}, which produces nonfunctional *Shaker* K^+ channels. Sh^{14} photoreceptors produced smaller voltage responses than wild-type photoreceptors when stimulated with identical white noise–contrast light stimuli (Fig. 2). This reduced response was seen in both the mean light-induced depolarization and the range of membrane potential fluctuations produced by dynamic stimuli. In the example shown here, a white noise stimulus with dynamic range approaching ±1 contrast units produced fluctuations of about 5 mV in the Sh^{14} photoreceptors, compared with more than 10 mV in the wild-type fly. Normal *Shaker* K^+ channels must therefore amplify the transduced signal amplitude, or add more uncorrelated noise to the membrane potential signal, or possibly both. Previous estimates of signal-to-noise ratios in wild-type and Sh^{14} photoreceptors, based on averaging responses to repeated stimuli, showed a strongly improved signal-to-noise ratio in wild-type photoreceptors, supporting the first hypothesis (Juusola and Hardie 2001a; Niven et al. 2003). However, that experimental approach could not separate uncorrelated noise from adaptive nonlinearities, and may thus have given biased estimates of the difference between wild-type and Sh^{14} photoreceptors. To study the nonlinear dynamic properties of wild-type and Sh^{14} photoreceptors, we estimated both linear and second-order nonlinear components of voltage responses using nonaveraged data.

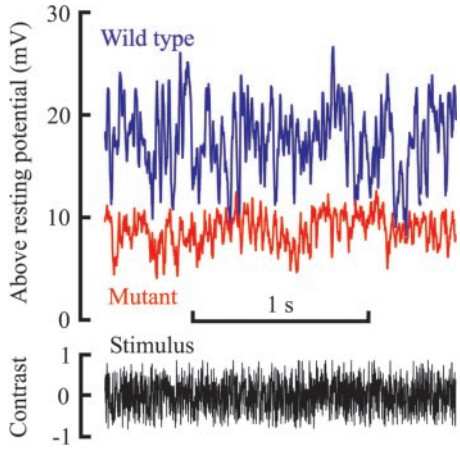

FIG. 2. Intracellularly recorded membrane potential responses of wild-type and Sh^{14} mutant photoreceptors to identical white noise–modulated light stimulus (*bottom panel*) for period of 2 s. Membrane potential responses are plotted as depolarization above resting potential on same axes. Note larger light-induced mean depolarization and larger fluctuating response of wild-type (blue) photoreceptor compared with Sh^{14} mutant (red).

Kernel estimates for photoreceptors

Preliminary measurements indicated that both first-order and second-order kernels extended for <60 ms along the time axes. Therefore all estimation and modeling was conducted using 30 lags of 2 ms. Parallel cascade fitting was used with cascade branches being added until the square of the residual error [$z(t)$ in Fig. 1] did not change after trying ≥100 new branches. Data are presented for three representative photoreceptors from each of the wild-type and Sh^{14} flies. The number of cascade branches required was approximately 20,000 for wild-type receptors and 100,000 for Sh^{14} photoreceptors (Table 1), with a mean cascade error of 25.4% for wild-type and 41.2% for Sh^{14}. These values reflect the relatively higher noise levels in Sh^{14} photoreceptors (Niven et al. 2003).

The MSE (*Eq. 2*) was calculated for the Volterra series (*Eq. 1*) using only K_0 and K_1 (MSE-K_1 in Table 1) and using all the kernels (MSE-K_2 in Table 1). Addition of the second-order kernel reduced MSE by about 2% in wild-type flies, and about 6% in Sh^{14} flies, indicating that there are nonlinear contributions to the responses of both animals, but that normal Sh^{14} K^+ channels confer more linear responses. MSE-K_2 values closely mirrored the cascade errors in all cases (note that these 2 errors were computed differently).

Kernel forms

Figure 3 shows kernel estimates from 3 representative wild-type photoreceptors. First-order kernels $K_1(u)$ had a repeatable form that was similar to flash responses in light-adapted *Drosophila* photoreceptors (Juusola and Hardie 2001a) with an initial delay of about 5 ms and a peak response at about 15 ms. Second-order kernels $K_2(u, v)$ also had a repeatable form, with a positive peak on the diagonal at about 12 ms and a negative, inhibitory peak at about 20 ms that spread away from either side of the diagonal by more than 5 ms. Plots of second-order kernel diagonals $K_2(u, u)$ are also shown in Fig. 3 (*bottom traces*). Note that the positive peak always occurred about 2 ms before the first-order kernel peak, and that the inhibitory peaks, which were clearly evident in the perspective plots, made little contribution to the kernel diagonal.

First-order kernels of *Shaker* mutant photoreceptors had very similar amplitudes and forms to those from wild-type flies (Fig. 4). However, the second-order kernels were dramatically different, with complete loss of the early positive peak and much clearer inhibitory peaks, which now dominated the diagonals (Fig. 4, *bottom traces*).

Predictions of photoreceptor output from the Volterra series (*Eq. 1*) were closely similar to the experimental values by eye. Examples for 2 s of the response from a wild-type receptor are shown in Fig. 5, both with and without the second-order kernel contributions. It was impossible to see the nearly 2% improvement in error contributed by $K_2(u, v)$ by eye.

NLN cascade model of phototransduction

Volterra series contain large numbers of parameters (496 in the present case). Attempts to convert these estimates to models with smaller numbers of parameters have concentrated on cascades of simple linear dynamic and nonlinear static components (French and Korenberg 1989; Korenberg and Hunter 1986). A model containing 2 static nonlinearities surrounding

TABLE 1. *Parallel cascade and NLN model-fitting errors*

Cascades	Cascade Error	MSE-K_1	MSE-K_2	MSE–NLN
Wild-type				
21,585	24.6	26.5	24.6	26.3
18,876	33.7	36.9	33.7	36.1
20,184	18.0	20.5	18.0	19.8
Sh^{14}				
90,861	61.5	65.7	61.5	62.8
123,184	34.5	42.3	34.5	35.9
123,547	27.7	33.3	27.7	28.9

a linear filter has been used before to reproduce the responses of photoreceptors to a wide range of stimuli (French et al. 1993) and the gamma function model (or Wong and Knight model) of photoreceptor function (Wong et al. 1980) has also been used in cascade models (Weckström et al. 1995). We combined these ideas to create the NLN model (Fig. 5 and *Eq. 3*) having only 8 variable parameters (see METHODS) to simulate the *Drosophila* photoreceptor responses.

Error values for the NLN model (MSE–NLN) were always intermediate between MSE-K_1 and MSE-K_2 (Table 1), indicating that the NLN model captured some, but not all, of the nonlinear photoreceptor behavior identified by the Volterra series. Expanding the polynomial functions to fourth-order did not reduce the error (data not shown). Fitted parameters for the same 3 wild-type and *Shaker* mutant photoreceptors are shown in Table 2 and plotted graphically in Fig. 7. Compared with wild-type flies, *Shaker* mutant parameters for the NLN model were different in two respects: *1*) a weaker second-order term made the polynomial function of the first static nonlinear component more linear, and *2*) the response of the linear component was slower and of smaller amplitude.

DISCUSSION

The contributions of *Shaker* K^+ channels to information processing in graded potential neurons are poorly understood. We compared the responses of wild-type and *Shaker* mutant (Sh^{14}) photoreceptors to white noise stimuli to characterize the dynamic nonlinear properties of the *Shaker* K^+ channels in *Drosophila* photoreceptors. Linear analysis did not reveal significant differences between the 2 photoreceptor types. However, nonlinear analysis revealed a positive nonlinearity that amplified the graded potential signal. This amplification is in contrast to the attenuation of voltage responses by *Shaker* K^+-channels in spiking neurons (Connor and Stevens 1971; Hoffman et al. 1997).

Fast, voltage-dependent ion channels in *Drosophila* photoreceptors change the membrane impedance and modify the frequency tuning of phototransduction (Juusola and Hardie 2001a; Niven et al. 2003). Flies with the Sh^{14} mutation differ from wild-type in the range of functional ion channels expressed in their photo-insensitive plasma membranes. The differences between the Volterra kernels obtained from wild-type and Sh^{14} photoreceptors probably reflect differences in these light-induced membrane impedance changes. How well can the known membrane properties and dynamics of wild-type and Sh^{14} photoreceptors explain the observed differences in the kernels?

Parallel cascade estimation gave consistent results for the Volterra kernels of phototransduction in both wild-type and Sh^{14} *Drosophila* photoreceptors. First-order kernels, representing the dominant linear contribution, were indistinguishable between wild-type and Sh^{14} flies, indicating that the basic phototransduction machinery and light current in *Shaker* mutants is intact. However, clear differences were seen in the

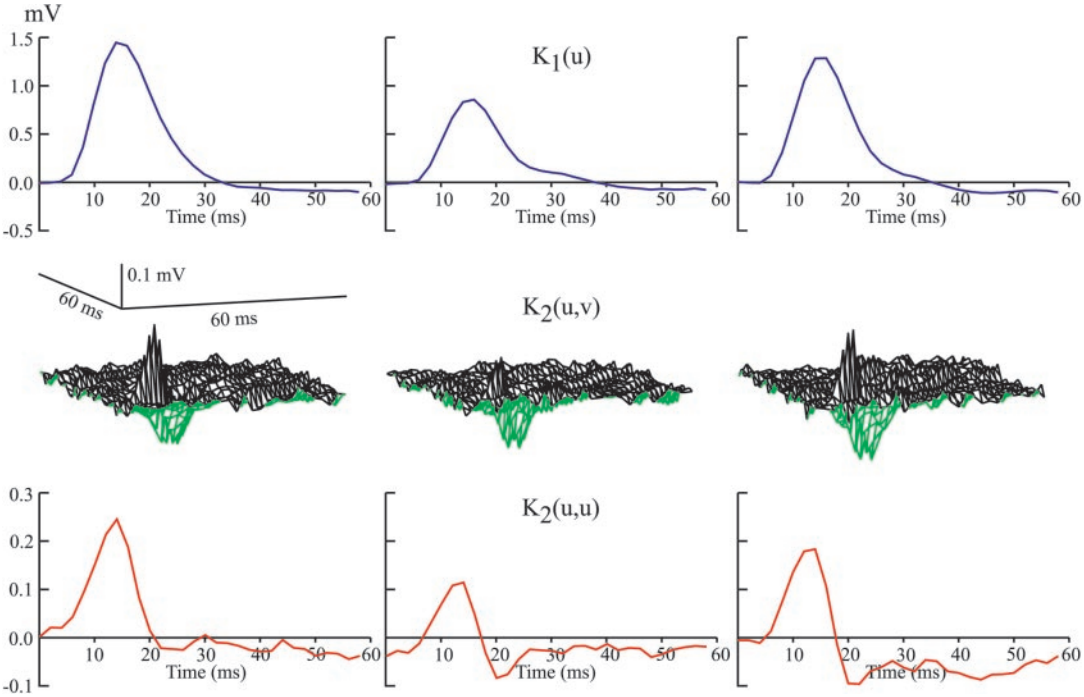

FIG. 3. First- and second-order kernels for phototransduction in three different wild-type *Drosophila* photoreceptors. *Top*: first-order kernels $K_1(u)$. *Middle*: perspective plots of second-order kernels $K_2(u, v)$. *Bottom*: diagonals of second-order kernels $K_2(u, u)$. Diagonal was always dominated by positive deflection, representing nonlinear amplification of signal during early phase of linear response. However, second-order kernel also showed significant, but later off-diagonal negative values.

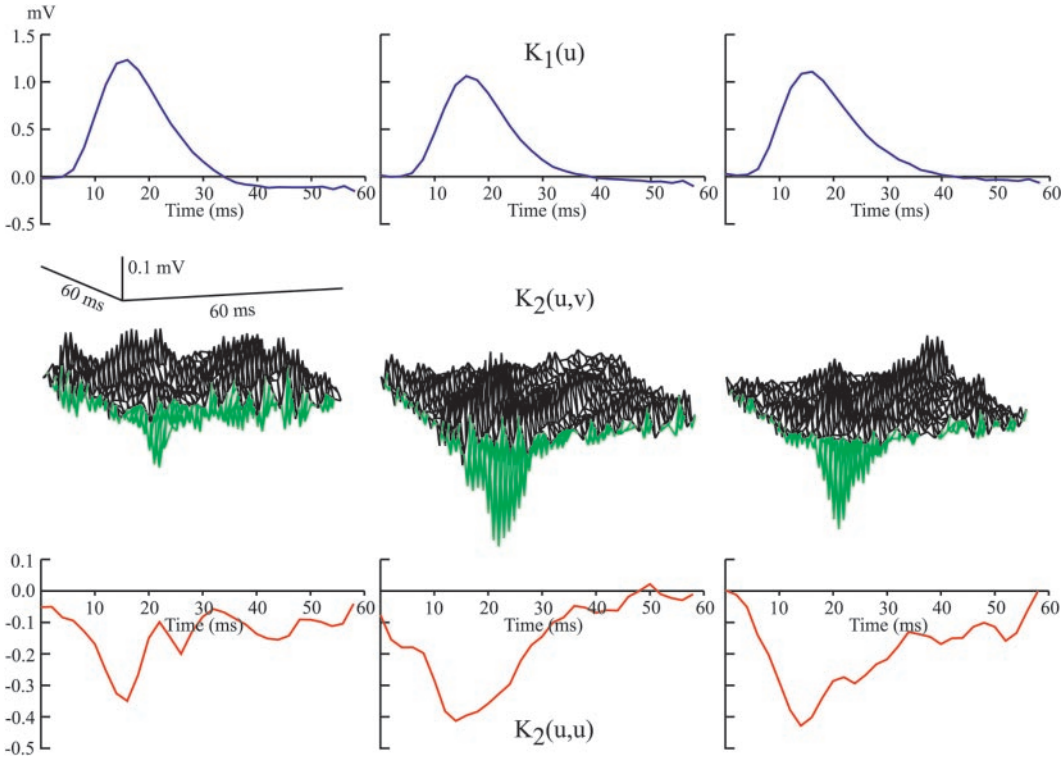

FIG. 4. First- and second-order kernels for phototransduction in three different photoreceptors of Sh^{14} mutant *Drosophila*. *Top:* first-order kernels $K_1(u)$. *Middle*: perspective plots of second-order kernels $K_2(u, v)$. *Bottom*: diagonals of second-order kernels $K_2(u,u)$. Positive peak in diagonal of second-order kernel was completely removed, and replaced by negative peak, continuous with slower and broader, off-axis negative values, having a similar distribution to those seen in wild-type receptors.

forms of the second-order kernels from wild-type and mutant flies, with the Sh^{14} photoreceptors lacking a major amplifying component that normally peaks during the rising phase of the response (Figs. 4 and 5), suggesting that *Shaker* K^+ channels mediate an amplification of the graded voltage signal that is absent from the Sh^{14} photoreceptors. This agrees with recent suggestions based on photoreceptor contrast gain functions, that *Shaker* K^+ channels normally amplify the voltage response in *Drosophila* photoreceptors (Niven et al. 2003).

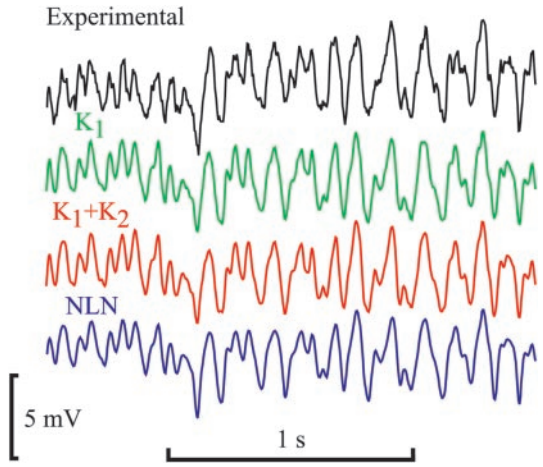

FIG. 5. Predicted photoreceptor responses of linear and nonlinear models. All traces are membrane fluctuations observed for period of 2 s. *Top*: experimental recording from wild-type receptor. *Second*: linear prediction based on measured value of $K_1(u)$ for this receptor and light input signal. *Third*: nonlinear prediction based on measured values of $K_1(u)$ and $K_2(u, v)$ for this receptor and light input signal. *Bottom*: prediction from NLN model (Fig. 6). These predictions were based on a section of experimental data that had not been used for model construction.

The time course of the second-order kernel in wild-type photoreceptors corresponds to the timing of the *Shaker* A-current I_A. The time constant of I_A, measured in dissociated wild-type photoreceptors by whole cell patch clamp, was 1.6 ± 0.3 ms at the resting membrane potential, and is likely to be faster in the depolarized state of our experiments at 25°C because the time-to-peak of I_A at 20 mV above rest was 1.3 ± 0.2 ms at 20°C (Hevers and Hardie 1995). We must also consider that the kernel results were not obtained from voltage or current pulse stimuli, but from white noise light stimulation where the membrane current response is delayed by the dead time of phototransduction (French 1980; Juusola and Hardie 2001b). It seems clear that the *Shaker* conductance, reflected in K_2, amplifies and accelerates the voltage response to light stimulation.

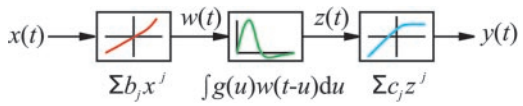

FIG. 6. NLN cascade model of phototransduction. Input light contrast signal $x(t)$ was assumed to pass through static nonlinearity, leading to linear, time-dependent filter and to final static nonlinearity. Intermediate signals were $w(t)$ and $z(t)$, and final output signal was $y(t)$. Static nonlinearities were modeled by third-order polynomial functions. Linear filter was Wong and Knight function of *Eq. 3*.

TABLE 2. *Fitted parameters of NLN cascade model*

First Polynomial		Wong and Knight Model			Second Polynomial		
c_2	c_3	n	τ (ms)	Offset	c_1 (mV)	c_2 (mV)	c_3 (mV)
Wild-type							
0.152	0.385	7.11	2.20	−0.003	17.24	−37.78	145.1
0.097	−0.043	8.32	1.84	−0.002	12.07	−18.91	−7.60
0.079	−0.114	8.36	1.79	−0.003	17.89	−23.81	45.67
Sh^{14}							
0.052	0.016	6.39	2.46	−0.004	20.53	−30.22	1.26
0.014	0.041	7.61	2.18	−0.002	16.08	−13.46	−2.40
0.039	0.057	5.88	2.68	−0.001	17.76	−17.70	5.67

Input signal was in dimensionless contrast units. Conversion to output in mV was assumed to occur in the second polynomial function. Parameter $c_1 = 1$ for the first polynomial function (see METHODS).

Photoreceptors with a *Shaker* null mutation also operate at much lower mean light-induced potentials than wild-type photoreceptors (Fig. 2). The lack of *Shaker* K^+ channels leads to a compensatory increase in leak conductance, as indicated by the reduced membrane impedance and higher dark resting potential of Sh^{14} photoreceptors (Niven et al. 2003), which probably causes the reduced response to light. The second-order kernels of Sh^{14} photoreceptors caused a significant gain reduction during the time course of the transduction seen in the first-order kernels, reflecting this voltage-dependent shunting.

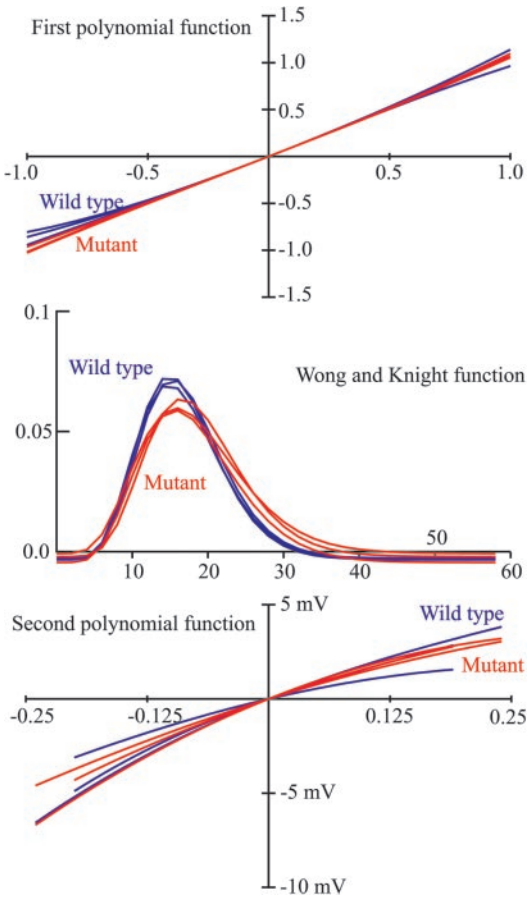

FIG. 7. Fitted components of NLN model of phototransduction for three wild-type (blue) and three Sh^{14} mutant (red) *Drosophila* photoreceptors. *Top*: first static nonlinearity was primarily a mild nonlinear compression of signal at negative contrast values. Compression was always greater for wild-type than for mutant receptors. *Middle*: linear filter for wild-type receptors was always faster and larger than for Sh^{14} photoreceptors. *Bottom*: second static nonlinearity showed significant compression with increasing response at all output values, but there were no detectable differences between wild-type and mutant receptors. Because linear amplification or attenuation can occur at any stage of a cascade, only parameters with absolute significance are dimensionless contrast input values along abscissa of top graph, and membrane potential output along ordinate of bottom graph.

The NLN cascade simulation, although clearly not adequate to account for all the nonlinear behavior, also suggested that *Shaker* K^+ channels increase the amplitude and speed of the phototransduction response (Fig. 7). The relatively small positive deviation in the first nonlinear component at negative contrasts has been reported before in another fly (*Calliphora*) photoreceptor (Weckström et al. 1995) and tentatively linked to fast voltage-activated K^+ channels. The reduction of this deviation in Sh^{14} photoreceptors indicates that there are differences between these two photoreceptor membranes in addition to the lack of *Shaker* K^+ channels in *Calliphora*. This difference probably arises from compensatory leak conductances (Niven et al. 2003), which partially offset the loss of *Shaker* K^+ channels in *Drosophila*, but are not equally present in *Calliphora* photoreceptors.

Kernel estimations in mutant flies gave much higher error levels than those in wild-type, supporting the idea that Sh^{14} photoreceptors have lower signal-to-noise ratios (Niven et al. 2003). Therefore it is difficult to estimate the relative contributions of nonlinearities and noise to changes in the coherence function because both reduce it (Bendat and Piersol 1980). However, here we have an independent measure of nonlinear contribution to the response by observing the reduction in MSE produced by adding the second-order kernel. Sh^{14} photoreceptors showed a greater reduction in MSE than that of their wild-type counterparts on addition of the second-order kernel (Table 1), indicating that *Shaker* K^+ channels partially linearize the normal photoreceptor voltage response. This linearizing effect of *Shaker* K^+ channels is supported by the forms of the 2 static nonlinear components in the NLN model (Fig. 7), where the form of the first nonlinear component in the wild-type flies would partly compensate for the opposite form of the third component, which was seen in all flies and is probably caused by membrane shunting.

What is the physiological role of the *Shaker* conductance in photoreceptors at bright light levels, which depolarize wild-type photoreceptors by approximately 20–25 mV above the dark resting potential ($E_m = -68.1 \pm 3.2$ mV, $n = 21$; Niven et al., 2003)? The majority of *Shaker* K^+ channels should be inactivated and therefore contribute relatively little to the photoreceptor membrane response. How-

ever, our results indicate that *Shaker* K^+ channels make significant contributions at depolarized potentials, both amplifying and accelerating the photoreceptor responses. This may be explained by the voltage separation of the steady-state activation and inactivation curves of the *Shaker* and delayed rectifier K^+ channels (Niven et al. 2003). Over a voltage range from -58 to -46 mV, depolarization decreases total steady-state K^+ conductance because *Shaker* channels are inactivating and relatively few delayed rectifier channels are activating. This reduction in total K^+ conductance amplifies the voltage signal. This model is supported by the loss of amplification and acceleration in the Sh^{14} mutant photoreceptors, which show a membrane shunt at high light intensities that is probably generated by activation of delayed rectifier K^+ channels. This effect would be masked in wild-type cells by *Shaker*-mediated amplification.

Are the effects of the Sh^{14} mutation entirely attributable to loss of functional *Shaker* channels in the photo-insensitive membrane? Sh^{14} has a missense mutation in the core region of the *Shaker* channel (Lichtinghagen et al. 1990). The effects of this mutation are not restricted to photoreceptors but have also been reported in motor neurons and muscles in both adults (Ganetzky and Wu 1982) and embryos (Broadie and Bate 1993; Haugland and Wu 1990). Sh^{14} affects circuits underlying flight and an escape response circuit (Engel and Wu 1992) as well as producing uncoordinated walking behavior (Ganetzky and Wu 1982) in adult flies. These effects all seem to be caused by loss of functional potassium channels in the neuromuscular system, rather than any pleiotropic effects. However, this does not exclude the possibility that elimination of functional *Shaker* channels has other effects on photoreceptor physiology. Additionally, if experience-dependent plasticity is important in developing normal photoreceptor function, it is possible that behavioral differences in Sh^{14} flies could in turn lead to different photoreceptor properties. However, this is unlikely to be a factor in the present study because all flies were reared in darkness.

An animal's lifestyle and behavior control the range and speed of natural stimuli it encounters, placing constraints and demands on the quality and processing capacity of its visual system. Laughlin (1996) suggested that slowly flying insects may use rapidly inactivating potassium conductances to create ohmic photoreceptor membranes under various light conditions. This metabolically inexpensive design, called matched filtering, would both maintain a high gain for relevant slow stimulus frequencies and filter out high-frequency phototransduction noise. However, our results suggest that the situation is not so simple, at least for the photoreceptors of relatively slow moving and turning *Drosophila*. Although *Drosophila* has poor spatial resolution with a small number of facets and blurred optics (Land 1997) its photoreceptors produce fast responses to constant variance light contrast stimuli. We found that the rapidly inactivating *Shaker* channels, instead of making the photoreceptor membranes ohmic act as nonlinear filters to accelerate and amplify phototransduction responses, and hence enhance the bandwidth of reliable signaling. The NLN model suggests that this amplification is an early nonlinearity that partly offsets later nonlinearities of opposite form.

DISCLOSURES

This work was supported by grants from the Canadian Institutes of Health Research to A. S. French, and the Royal Society, Wellcome Trust, and Biotechnology and Biological Sciences Research Council to M. Juusola.

REFERENCES

Bendat JS and Piersol AG. *Engineering Applications of Correlation and Spectral Analysis.* New York: Wiley, 1980, p. 1–302.

Broadie KS and Bate M. Development of larval muscle properties in the embryonic myotubes of *Drosophila melanogaster. J Neurosci* 13: 167–180, 1993.

Connor JA and Stevens CF. Voltage clamp studies of a transient outward membrane current in gastropod neural somata. *J Physiol* 213: 21–30, 1971.

Debanne D, Guerineau NC, Gahwiler BH, and Thompson SM. Action-potential propagation gated by an axonal I(A)-like K^+ conductance in hippocampus. *Nature* 389: 286–289, 1997.

Engel JE and Wu CF. Genetic dissection of functional contributions of specific potassium channel subunits in habituation of an escape circuit in *Drosophila. J Neurosci* 18: 2254–2267, 1998.

French AS. Phototransduction in the fly compound eye exhibits temporal resonances and a pure time delay. *Nature* 283: 200–202, 1980.

French AS and Korenberg MJ. A nonlinear cascade model for action potential encoding in an insect sensory neuron. *Biophys J* 55: 655–661, 1989.

French AS, Korenberg MJ, Järvilehto M, Kouvalainen E, Juusola M, and Weckström M. The dynamic nonlinear behavior of fly photoreceptors evoked by a wide range of light intensities. *Biophys J* 65: 832–839, 1993.

French AS and Marmarelis VZ. Nonlinear analysis of neuronal systems. In: *Modern Techniques in Neuroscience Research*, edited by Windhorst U and Johansson H. Berlin: Springer-Verlag, 1999, p. 627–640.

French AS, Sekizawa S, Höger U, and Torkkeli PH. Predicting the responses of mechanoreceptor neurons to physiological inputs by nonlinear system identification. *Ann Biomed Eng* 29: 187–194, 2001.

Ganetzky B and Wu CF. Indirect suppression involving behavioral mutants with altered nerve excitability in *Drosophila melanogaster*. *Genetics* 100: 597–614, 1982.

Hardie RC. Voltage-sensitive potassium channels in *Drosophila* photoreceptors. *J Neurosci* 11: 3079–3095, 1991.

Hardie RC. Phototransduction in *Drosophila melanogaster*. *J Exp Biol* 204: 3403–3409, 2001.

Haugland FN and Wu CF. A voltage-clamp analysis of gene-dosage effects of the *Shaker* locus on larval muscle potassium currents in *Drosophila. J Neurosci* 10: 1357–1371, 1990.

Hevers W and Hardie RC. Serotonin modulates the voltage dependence of delayed rectifier and Shaker potassium channels in *Drosophila* photoreceptors. *Neuron* 14: 845–856, 1995.

Hille B. *Ionic Channels of Excitable Membranes.* Sunderland, MA: Sinauer Associates, 2001, p. 1–814.

Hoffman DA, Magee JC, Colbert CM, and Johnston D. K^+ channel regulation of signal propagation in dendrites of hippocampal pyramidal neurons. *Nature* 387: 869–875, 1997.

Juusola M and Hardie RC. Light adaptation in *Drosophila* photoreceptors: II. Rising temperature increases the bandwidth of reliable signaling. *J Gen Physiol* 117: 27–42, 2001a.

Juusola M and Hardie RC. Light adaptation in *Drosophila* photoreceptors. I. Response dynamics and signaling efficiency at 25 degrees C. *J Gen Physiol* 117: 3–25, 2001b.

Kaplan WD and Trout WE. The behavior of four neurological mutants of *Drosophila. Genetics* 61: 399–409, 1961.

Kitano H. Computational systems biology. *Nature* 420: 206–210, 2002.

Korenberg MJ and Hunter IW. The identification of nonlinear biological systems: LNL cascade models. *Biol Cybern* 55: 125–134, 1986.

Korenberg MJ. Parallel cascade identification and kernel estimation for nonlinear systems. *Ann Biomed Eng* 19: 429–455, 1991.

Land MF. Visual acuity in insects. *Annu Rev Entomol* 42: 147–177, 1997.

Laughlin SB. Matched filtering by a photoreceptor membrane. *Vision Res* 36: 1529–1541, 1996.

Laurent G. Voltage-dependent nonlinearities in the membrane of locust nonspiking local interneurons, and their significance for synaptic integration. *J Neurosci* 10: 2268–2280, 1990.

Lichtinghagen R, Stocker M, Wittka R, Boheim G, Stuhmer W, Ferrus A, and Pongs O. Molecular basis of altered excitability in *Shaker* mutants of *Drosophila melanogaster. EMBO J* 9: 4399–4407, 1990.

Magee JC, Hoffman DA, Colbert C, and Johnston D. Electrical and calcium signaling in dendrites of hippocampal pyramidal neurons. *Annu Rev Physiol* 60: 327–346, 1998.

Niven JE, Vähäsöyrinki M, Kauranen M, Hardie RC, Juusola M, and Weckström M. The contribution of *Shaker* K(+) channels to the information capacity of *Drosophila* photoreceptors. *Nature* 421: 630–634, 2003.

Press WH, Flannery BP, Teukolsky SA, and Vetterling WT. *Numerical Recipes in C. The Art of Scientific Computing.* Cambridge, UK: Cambridge Univ. Press, 1990, p. 1–735.

Schilstra C and van Hateren JH. Blowfly flight and optic flow. I. Thorax kinematics and flight dynamics. *J Exp Biol* 202: 1481–1490, 1999.

van Hateren JH and Schilstra C. Blowfly flight and optic flow. II. Head movements during flight. *J Exp Biol* 202: 1491–1500, 1999.

Weckström M, Juusola M, Uusitalo RO, and French AS. Fast-acting compressive and facilitatory nonlinearities in light-adapted fly photoreceptors. *Ann Biomed Eng* 23: 70–77, 1995.

Weckström M and Laughlin SB. Visual ecology and voltage-gated ion channels in insect photoreceptors. *Trends Neurosci* 18: 17–21, 1995.

Wong F, Knight BW, and Dodge FA. Dispersion of latencies in photoreceptors of *Limulus* and the adapting bump model. *J Gen Physiol* 76: 517–537, 1980.